J Mater Sci (2015) 50:2903–2913
DOI 10.1007/s10853-015-8854-y

Zirconium-methacrylate oxoclusters as new hybrid materials for the modification of epoxy systems

Bluma G. Soares · Shalimar Caplan · Sébastien Livi · Alexandre Gatti · Sidney J. L. Ribeiro

Received: 27 October 2014 / Accepted: 12 January 2015 / Published online: 27 January 2015

Abstract Oxozirconium clusters bearing methacrylate moiety (ZrMe) were synthesized by sol–gel process and used in epoxy networks to develop epoxy-based nanocomposites with potential application as encapsulant for light-emitting diode. Diglycidyl ether of bisphenol A-based epoxy resin was previously functionalized with acrylic acid to introduce some vinyl groups in the matrix and improve its interaction with the oxocluster. The ZrMe particles were previously dispersed in the epoxy matrix or in the 4-methyl-tetrahydrophthalic anhydride used as hardener, and the systems were cured with anhydride or with a combination of anhydride and benzoyl peroxide. The last compound promotes the covalent bond between the epoxy matrix and the ZrMe through free radical reactions between the vinyl groups. The dispersion of ZrMe into the epoxy matrix resulted in a significant increase in viscosity, mainly for systems dispersed with a combination of high shear mechanical mixing and ultrasonification. The dispersion of ZrMe into the anhydride resulted in nanocomposites with higher transparency, better dispersion of the oxocluster into the matrix bulk, as observed by transmission electron microscopy, and higher thermal conductivity, mainly for systems cured with anhydride and peroxide. The use of anhydride in combination with BPO also resulted in significant increase in glass transition temperature.

B. G. Soares (✉) · S. Caplan
Universidade Federal do Rio de Janeiro, Instituto de Macromoléculas, Centro de Tecnologia, Bl. J, Ilha do Fundão, Rio de Janeiro, RJ 21941-598, Brazil
e-mail: bluma@ima.ufrj.br

S. Livi
Université de Lyon, 69003 Lyon, France

S. Livi
INSA Lyon, 69621 Villeurbanne, France

S. Livi
CNRS, UMR 5223, Ingénierie des Matériaux Polymères, Villeurbanne, France

A. Gatti · S. J. L. Ribeiro
Instituto de Química – UNESP, Araraquara, SP 14801-970, Brazil

Introduction

Epoxy resins are one of the most commonly used engineering thermosets because of their good mechanical performance, thermal stability, chemical resistance, and adhesion properties [1]. The incorporation of inorganic particles into the epoxy resins has attracted significant interest as a way to achieve a synergetic combination of typical properties of each component. However, the distribution of such particles in the polymer matrix is a key parameter which can be solved by developing new organic–inorganic hybrid materials constituted by inorganic core surrounded by organic segments with appropriated functional groups able to provide better compatibilization with the organic polymer matrix [2–5]. The success of this field is mainly assigned to the possibility of preparing inorganic structures by using the soft chemistry approach, also known as "chimie douce," such as the sol–gel processing [6]. Among several inorganic particles used to modify epoxy systems, zirconia appears as a very promising inorganic component to impart some specific characteristics such as, high refractive index, large optical band gap, and low optical loss [7]. These properties associated with high transparency are very important for encapsulating light-emitting diodes (LEDs), because they are able to reduce the refractive index mismatch between the LED dies and air [8, 9]. Different approaches have been reported

for the development of epoxy/zirconia hybrid materials. Medina et al. [10] used commercial zirconium dioxide (ZrO_2) nanoparticles in epoxy matrix cured with cyclic aliphatic amine and found an improvement of modulus. However, the particles form aggregates resulting in opaque materials. Sajjad et al. [11] prepared ZrO_2 nanoparticles through hydrothermal conditions and modified them with functionalized diethylene glycol to increase the compatibility with epoxy matrix. The authors obtained homogeneous and transparent materials with the addition of 2.34 vol% of ZrO_2. Bondioli et al. [12] prepared sub-micron spherical zirconia particles by sol–gel process and used as reinforcing agents for epoxy networks, obtaining an increase of Young modulus. Such particles also improved the adhesion properties of epoxy-based adhesives but the resulting hybrid materials are opaque, indicating a strong tendency for particle aggregation [13]. To avoid the particle aggregation phenomenon, some authors performed the in situ generation of ZrO_2 in the presence of epoxy matrix through the sol–gel procedure. Ochi et al. [14–16] and Bondioli et al. [17] employed this strategy to prepare homogeneous epoxy/zirconia hybrid materials. The sol–gel process of the alkoxide zirconium inside the epoxy matrix was performed in the presence of acetic acid [14, 15], hexahydrophthalic anhydride [16] or acetyl acetone [17] to control the hydrolysis/condensation reactions. Epoxy/ZrO_2 nanocomposite was also reported by Chung et al. [18] using silane-modified ZrO_2 fillers. The zirconia particles were previously prepared by the precipitation of zirconyl chloride using methacrylic acid and triethanolamine as chelating agents. The particles were modified with functionalized silanes to improve the compatibilization with the epoxy matrix. Such materials were tested as encapsulants for different types of LED packages. ZrO_2/epoxy nanocomposites with high transparency and high refractive index for LED encapsulation were recently developed by Tao et al. [9]. In order to improve the interaction between the inorganic phase and the epoxy matrix, the authors synthesized ZrO_2 particles using benzyl alcohol as the chelating agent to decrease the reactivity of the zirconium alkoxide toward the sol–gel reaction, followed by a treatment of the particles with (3-glyciloxypropyl) trimethylsilane. The nanocomposite obtained by this process displayed high transparency and an increase of the refractive index.

Oxozirconium clusters bearing (meth)acrylate groups have been prepared by Schubert et al. [19, 20], through the sol–gel process involving the hydrolysis/condensation of tetraalkoxyzirconium in the presence of excess of (meth) acrylic acid. These carboxylic acids act as bidentate ligands, decreasing the reactivity of the sol–gel process. Additionally, they are able to control the size of the primary clusters and introduce functionalized/polymerizable groups at the cluster surface.

The present paper describes for the first time the preparation of epoxy/zirconia hybrid networks using methacrylate-substituted oxozirconium cluster aiming to develop new transparent materials to be employed as encapsulating materials for LEDs as well as other electro-electronic applications. The motivation of using this functionalized oxozirconium cluster in epoxy systems was based on the well-known affinity of methyl methacrylate and its polymer with epoxy resin. Therefore, the methacrylate moiety located at the surface of the zirconium oxocluster can act as a compatibilizer between the inorganic component and the epoxy matrix. In order to increase the interaction between the components, epoxy matrix was previously functionalized with acrylic acid. Benzoyl peroxide (BPO) was also employed to perform the covalent bond between the functionalized cluster and epoxy resin through free radical addition.

Experimental

Materials

Diglycidyl ether of bisphenol A (DGEBA) (ER)-based epoxy pre-polymer (EPON 828) (epoxy equivalent weight = 188–192; viscosity = 110–150 P; molar mass ≈ 377; hydroxyl groups ≈ 0.05 mol/100 g) was purchased from Shell Chemicals do Brasil. 4-Methyl-tetrahydrophthalic anhydride (MTHPA) (Aradure HY2123) was supplied by Huntsmann. Both epoxy pre-polymer and anhydride were dried under reduced pressure at 80 °C for about 4 h, before using. Methacrylic acid from Lucite™, triphenylphosphine and acrylic acid (Merck), zirconium *n*-propoxide in a 70 % solution in n-propanol (Tyzon NPZ) from Dupont, and BPO from Sigma-Aldrich were employed without purification.

Synthesis of zirconium-methacrylate oxocluster

Zirconium-methacrylate oxocluster (ZrMe) used in this work was synthesized according to the procedure described in the literature [21]. In a typical procedure, 0.05 mol of zirconium *n*-propoxide in a 70 % solution in *n*-propanol was mixed with 0.35 mol of methacrylic acid under nitrogen atmosphere. The mixture was stored under nitrogen at room temperature for 1 week. The precipitated crystals were filtered and dried at 60 °C for 24 h.

Functionalization of epoxy pre-polymer with acrylic acid (ER-AA)

Epoxy pre-polymer was functionalized with acrylic acid to improve its compatibility with the ZrMe oxoclusters. The

reaction was performed by stirring ER with 1 wt% (2.64 mol%) of acrylic acid (related to the amount of ER) and 0.1 % of triphenylphosphine as the catalyst, at 80 °C for 1 h under nitrogen atmosphere. After the reaction, the non-reacted acrylic acid was removed under reduced pressure at 100 °C for 24 h. The functionalization of ER, according to the scheme illustrated in Fig. 1, was confirmed by the appearance of an absorption band in the Fourier transform infrared (FTIR) spectrum at 1730 cm^{-1}, assigned to the carbonyl stretching vibration of the acrylate moiety.

Preparation of the ER-AA/ZrMe cluster dispersion and curing process

ZrMe oxocluster was dispersed in the functionalized DGEBA (ER-AA) matrix or in the anhydride used as the hardener. For the ER-AA/ZrMe dispersions, pre-established amount of ZrMe was dissolved in a small amount of acetone. Then, the ER-AA was added and the system was dispersed using different procedures as summarized in Table 1. After the dispersion, the acetone was removed under reduced pressure at 70 °C, and a stoichiometric amount of anhydride was added and gently mixed to avoid bubbles. In another curing system, BPO (1 wt% related to the oxocluster) was also added in some mixtures in this step to impart the reaction between the double bonds of the oxocluster and the modified epoxy resin. The system was degassed under reduced pressure, casted into silicone molds, and submitted to the curing process using the following protocol: 3 h at 80 °C, 2 h at 110 °C, and 1 h at 130 °C.

The dispersion of ZrMe in the anhydride was performed without the addition of acetone using the methodology described in Table 1 (method *IV*). After the dispersion, the ER-AA was added and the system was degassed under reduced pressure, casted into silicone molds, and cured under the same conditions as previously described. For systems containing BPO, it was added immediately after the addition of the ER-AA.

Characterization

Fourier transformed Infrared spectrum (FTIR) of the zirconium oxocluster was recorded from KBr on a Nicolet iS50 spectrometer in a transmission mode (32 scans, resolution of 4 cm^{-1}), in the wavelength range from 4000 to 500 cm^{-1}.

Thermogravimetric analysis of the zirconium-based oxocluster was performed on a Q50 thermobalance from TA Instruments Inc. The samples were heated from 30 to 750 °C, at a heating rate of 10 °C/min, under nitrogen flow.

The rheology of the dispersions was carried out using a Physica MRC302 rheometer from Anton Paar, disposed with parallel-plates with 20 mm diameter and a gap of 500 μm at 25 °C.

Dynamic mechanical analyzer (Q-800, TA Scientific) was used for measuring dynamic mechanical properties of cured epoxy networks at a fixed frequency of 1 Hz with a heating rate of 3 °C/min. A single cantilever clamp was used.

Transmission electron microscopy (TEM) was carried out at the Technical Center of Microstructures (University of Lyon) on a Phillips CM 120 microscope operating at 80 kV to characterize the distribution of nanoparticles in the epoxy matrix. The samples were cut using an ultramicrotome equipped with a diamond knife, to obtain 60-nm-thick ultrathin sections. Then, the sections were set on copper grids.

The optical transparency was obtained using a Varian-Cary 100 UV–visible spectrometer in the range of 400–800 nm. The epoxy or the corresponding ER-AA/ZrMe was blended with the curing agent and applied onto microscope glasses by roll-coating (film thickness of about 80 μm). Then, the samples were cured using the same curing protocol as described before.

The thermal conductivity was performed on a Nano Flash LFA 447 from Netzsch which measures the thermal diffusivity (α [mm^2/s]). Heat pulses irradiate from a Xenonium lamp on the front side of sample (dimension = 13 × 13 × 0.5 mm), and the heat transmitted is measured by an infrared camera. The equipment operates in the range of 0.001–10 cm^2/s.

The thermal conductivity (W/(m K) is determined from the Eq. 1:

$$k = \propto \rho c_p, \quad (1)$$

where k is the thermal conductivity, α is the thermal diffusivity (m^2/s), ρ is the density (kg/m^3), and c_p is the specific heat (J/(kg K)), which was determined from differential scanning calorimetry measurements. The density was considered as that of pure epoxy network ($\rho = 1.2$ kg/m^3) since low amount of ZrMe was employed in these systems.

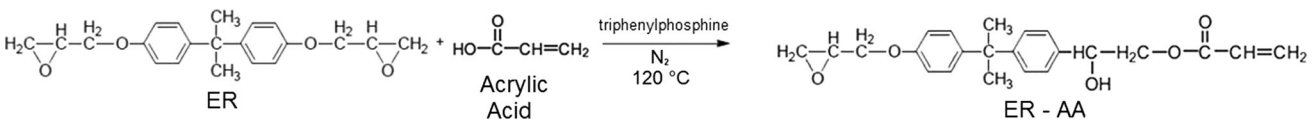

Fig. 1 Reaction between the epoxy resin and acrylic acid

Table 1 Methodology used for the preparation of ZrMe-based dispersions

Method	Dispersion medium	Dispersion procedure
I	ER-AA/acetone	High shear mechanical mixing (IKA model T25) at 17500 rpm for 25 min.
II	ER-AA/acetone	Three steps of sonication using a Sonifier® S-450D digital Branson ultrasonic apparatus operating at 40 Watts for 10 min each step.
III	ER-AA/acetone	High shear mechanical mixing (IKA model T25) at 17500 rpm for 25 min followed by two steps of sonication using a Sonifier® S-450D digital Branson ultrasonic apparatus operating at 40 Watts for 10 min each step
IV	Anhydride	Similar dispersion procedure as method *III*

The refractive index was determined with an m-line apparatus (Metricon mod. 2010) based on the prism coupling technique with a He–Ne laser operating at 543.5 nm.

Results and discussion

Characterization of the zirconium-methacrylate oxocluster (ZrMe)

The ZrMe oxocluster was characterized by FTIR and TGA, whose results are illustrated in Fig. 2 (left and right, respectively). The TGA curve presents two well-defined degradation steps: the first one in the temperature range 100–200 °C may be ascribed to the degradation of physically adsorbed methacrylic acid, as also suggested by Trimmel et al. [21]. The second step in the range of 200–600 °C is attributed to the complete decomposition of the methacrylate complex [9, 21]. Similar profile was reported by Trimmel et al. [21] for the degradation of $Zr_4O_2(OMc)_{12}$, confirming the presence of the ZrMe oxocluster. The weight loss between 200 and 600 °C corresponds to around 34 wt% of methyl methacrylate moiety, which is in agreement with that result reported by Trimmel et al. [21].

The presence of methacrylate as the organic moiety in the hybrid was confirmed by FTIR. The broad absorption at around 3400 cm^{-1} (peak a) is related to the OH stretching vibration. The intense peaks at 1555 cm^{-1} (peak b) and 1422 cm^{-1} (peak c) correspond to asymmetric and symmetric vibration of the carboxylate ligand of the methacrylate moiety, respectively. These absorptions confirm the formation of chemical bond between the carboxylate groups of methacrylic acid and the Zr–OH site at the ZrO_2 surface as a bidentate ligand [14, 22, 23]. Also the bands at 1637 cm^{-1}, (peak d) assigned to the C=C stretching vibration, 940 cm^{-1} (peak e) attributed to the Zr–OC stretching vibrations and at 660 cm^{-1} (peak f), ascribed to the Zr–O bending vibration, confirm the structure of the hybrid in the form of cluster of methacrylate linked to the zirconium core particles.

Influence of the dispersion procedure on the main properties of ER-AA/ZrMe nanocomposites

Rheological properties of the ER-AA/zirconium-methacrylate oxocluster dispersions

The dependence of the complex viscosity with the shear rate for the ER-AA/ZrMe oxocluster dispersions containing

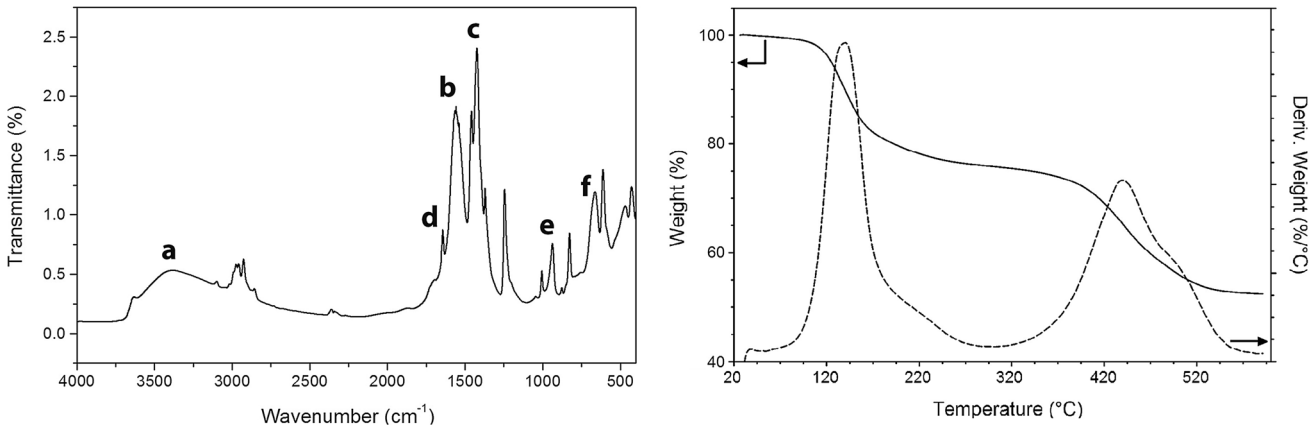

Fig. 2 FTIR spectrum and TGA curve of the ZrMe oxocluster

5 phr of ZrMe and prepared by different procedures (as summarized in Table 1) is presented in Fig. 3. The presence of ZrMe resulted in a significant increase in viscosity, related to the pure ER-AA matrix, and the highest viscosity response was observed for the dispersion prepared by method *III* (which combines high shear mechanical mixing and ultrasound tip). This is an indication of better interaction between the ZrMe oxocluster and the ER-AA matrix due to the increase of the interfacial area promoted by the better dispersion and consequently a decrease of the particle size.

To better analyze the rheological behavior of the dispersions, the data were fitted to the Ostwald-de Waele power law equation:

$$\tau = K \cdot \dot{\gamma}^n, \quad (2)$$

where K is the flow consistency index and n is the flow behavior index.

Figure 4 illustrates the dependence of the shear stress with shear rate. The experimental data were well fitted to the theoretical model, making possible the calculation of the main rheological parameters, whose values are summarized in Table 2. The index n is related with the pseudoplasticity of the dispersion. The epoxy matrix presents n value close to the Newtonian behavior. The ER-AA/ZrMe dispersions prepared by the methods *I* and *II* present slight deviation from the Newtonian behavior, presenting n values of 0.96 and 0.98, respectively. On the other hand, the dispersion prepared by method *III* resulted in lower n value, suggesting a shear-thinning behavior in larger extent, that is, a decrease in viscosity with increasing the shear rate. This phenomenon, also observed in Fig. 3, occurs at higher shear rate and is generally explained by rotation and alignment effects of the nanoparticles induced by the shear flow field [24]. Such shear-thinning characteristic is commonly observed in well-dispersed systems because the nanoparticles require lower energy to rotate and align toward the shear direction [25, 26].

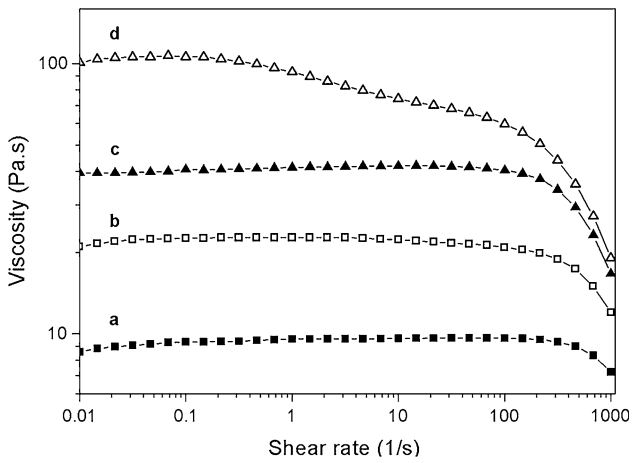

Fig. 3 Dependence of the complex viscosity with shear rate for the (*a*) ER-AA pre-polymer and the ER-AA/ZrMe oxocluster dispersions performed by (*b*) method *I*; (*c*) method *II*; and (*d*) method *III*

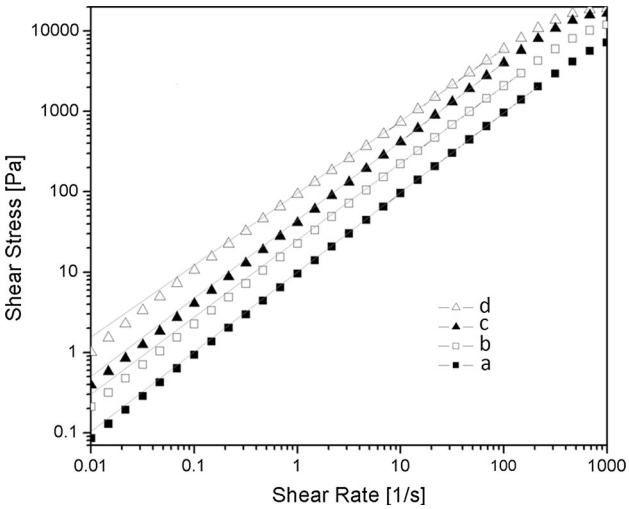

Fig. 4 Dependence of the shear stress with shear rate for the (*a*) ER-AA pre-polymer and the ER-AA/ZrMe oxocluster dispersions performed by (*b*) method *I*; (*c*) method *II*; and (*d*) method *III*. (The *solid lines* correspond to the theoretical dependence based on the power law equation)

Table 2 Main rheological parameter obtained from the power law equation for the ER-AA/ZrMe dispersions prepared by different procedures

Sample	Dispersion method	η_0	n	K	R
ER-AA	–	8.6	0.99	9.99	0.9995
EE-AA/ZrMe	Method *I*	21.0	0.96	24.96	0.9996
EE-AA/ZrMe	Method *II*	39.4	0.98	45.09	0.9994
EE-AA/ZrMe	Method *III*	101.0	0.89	96.73	0.9992

Influence of the dispersion procedure on the viscoelastic properties of ER-AA/ZrMe nanocomposites

The effect of the dispersion method on the dynamic mechanical properties of ER-AA/ZrMe nanocomposites is illustrated in Fig. 5. For this study, 5 phr of ZrMe was previously dispersed inside the ER-AA matrix and cured with anhydride. All ER-AA/ZrMe nanocomposites display higher storage modulus than pure epoxy network, indicating an improvement of the mechanical strength of the system promoted by the ZrMe oxocluster. The nanocomposites whose ZrMe was previously dispersed by method *III* display the highest modulus, highlighting the importance of the oxocluster dispersion on the reinforcement of

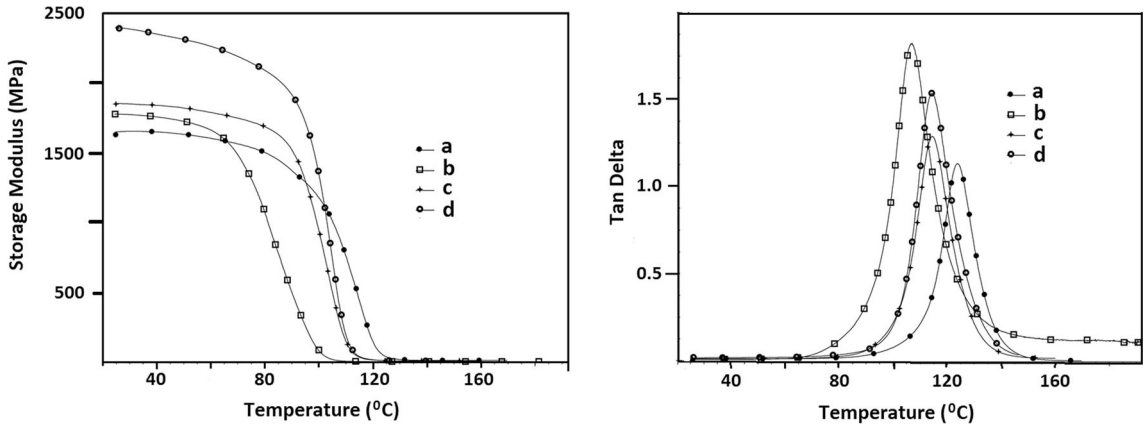

Fig. 5 Dependence of the storage modulus and tan delta with temperature for (*a*) ER network and the ER-AA/ZrMe oxocluster networks whose dispersion was performed by (*b*) method *I*; (*c*) method *II*; and (*d*) method *III*

the epoxy matrix by the ZrMe oxocluster. The presence of the ZrMe resulted in a decrease of the glass transition temperature (α-transition) probably because of the increasing in the free volume at the filler–matrix interface. Additionally, the decrease of the T_g may be also related to the mobility of the methacrylate moiety located at the ZrMe oxocluster surface.

Effect of ZrMe content on the main properties of ER-AA/ZrMe nanocomposites

Rheological properties of ER-AA/ZrMe dispersions

The effect of the ZrMe content on the rheological behavior of ER-AA/ZrMe dispersions is illustrated in Fig. 6, in terms of viscosity and shear stress as a function of the shear rate. For this study, the method *III* was used for dispersing the ZrMe inside the ER-AA matrix. The modification of ER with acrylic acid does not exert any influence on the rheological properties, indicating that no polymerization or crosslink reaction involving the double bonds of the EE-AA occurred during the functionalization and purification steps. As expected, the viscosity increases with the amount of ZrMe. The ER-AA/ZrMe dispersion containing 1 phr of the ZrMe presents viscosity 100 % higher than the pure ER-AA, indicating an effective interaction between filler and matrix. All compositions present shear-thinning behavior at higher shear rate, which is more significant for system containing 5 phr of ZrMe.

Properties of the cured ER-AA/ZrMe nanocomposites

For the studies related to the cured ER-AA/ZrMe nanocomposites, the ZrMe cluster was previously dispersed in the ER-AA matrix using method *III* or in the anhydride using method *IV*.

Morphological behavior All networked materials presented excellent optical transparency, regardless the dispersion method and the curing system. To reveal the structure of these hybrid materials and their distribution in the epoxy matrix, the TEM was employed for samples containing 5 phr of ZrMe oxocluster, whose micrographs are illustrated in Fig. 7. In spite of excellent optical transparency, the systems prepared by method *III* (ZrMe previously dispersed in epoxy matrix) present the ZrMe oxoclusters dispersed in the form of elongated flakes with less than 10 nm in diameter and some aggregates. The use of BPO in combination with anhydride imparts better dispersion of these aggregates (Fig. 7b). The previous dispersion of ZrMe in the anhydride (method *IV*) resulted in very homogeneous systems. Very few aggregates and some few tubes can be seen in the nanocomposite cured with anhydride (Fig. 7c), whereas no visible particle can be observed in the system cured with the anhydride/BPO (Fig. 7d), suggesting almost miscibility of the oxocluster probably because of the formation of chelates between anhydride and the oxocluster as previously mentioned, and also the formation of covalent bond between the double bonds of the meth(acrylate) moieties located on the ER-AA chain and at the ZrMe oxocluster surface, through free radical reaction, as illustrated in Fig. 8.

Optical properties Transparency of thin films constitutes important characteristics to determine the applications as LED encapsulating and other opto-electronic devices. Although all hybrid materials are very transparent, this property was quantified by UV–Vis spectroscopy, whose spectra are illustrated in Fig. 9. The transmittance of all materials stays above 85 %, in the range of 450–800 nm, confirming the excellent optical transparency. The transparency decreases as the amount of ZrMe increases. However, for the same ZrMe content, the ER-AA/ZrMe

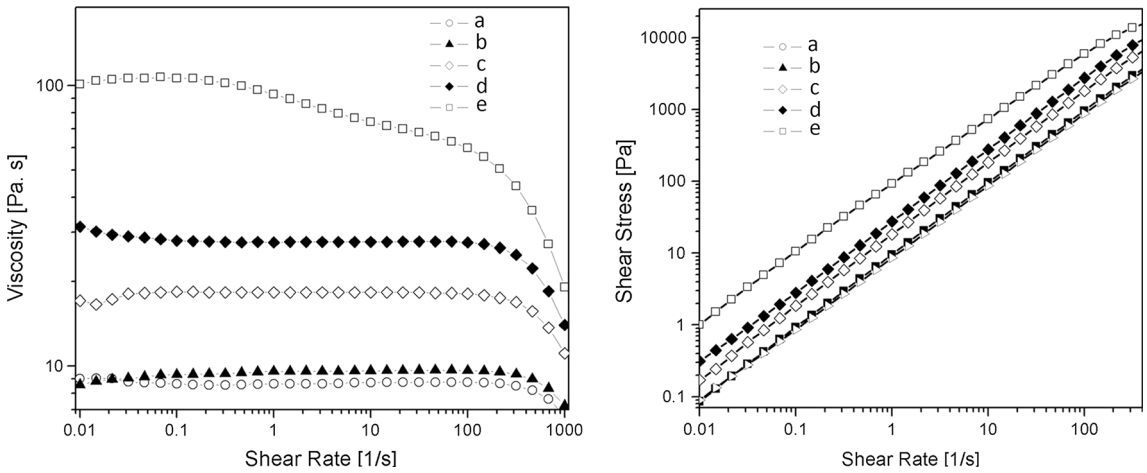

Fig. 6 Dependence of the complex viscosity and shear stress with shear rate for the (*a*) ER; (*b*) ER-AA pre-polymer and the ER-AA/ZrMe oxocluster dispersions containing (*c*) 1 phr; (*d*) 3 phr; and (*e*) 5 phr of the ZrMe

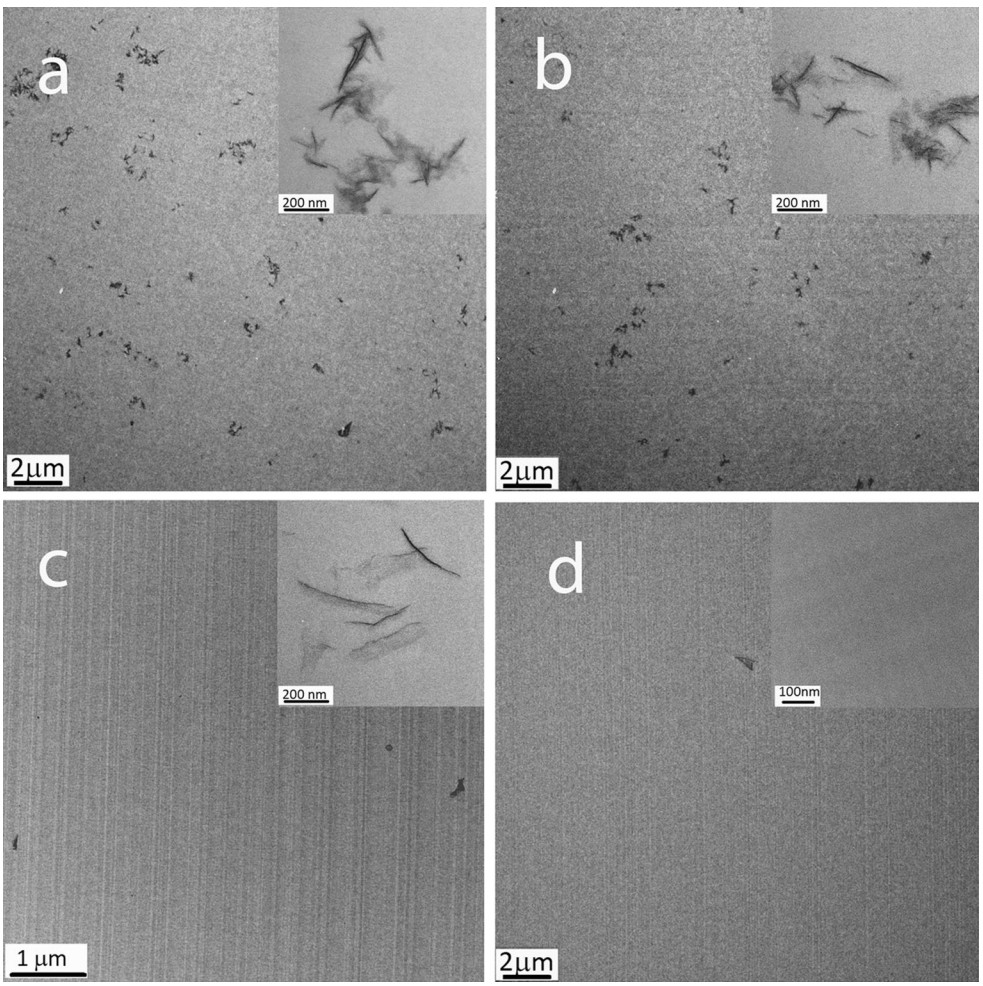

Fig. 7 TEM micrographs of ER-AA/ZrMe nanocomposites prepared by **a** method *III*, cured with anhydride; **b** method *III*, cured with anhydride/BPO; **c** method *IV*, cured with anhydride; **d** method *IV*, cured with anhydride/BPO

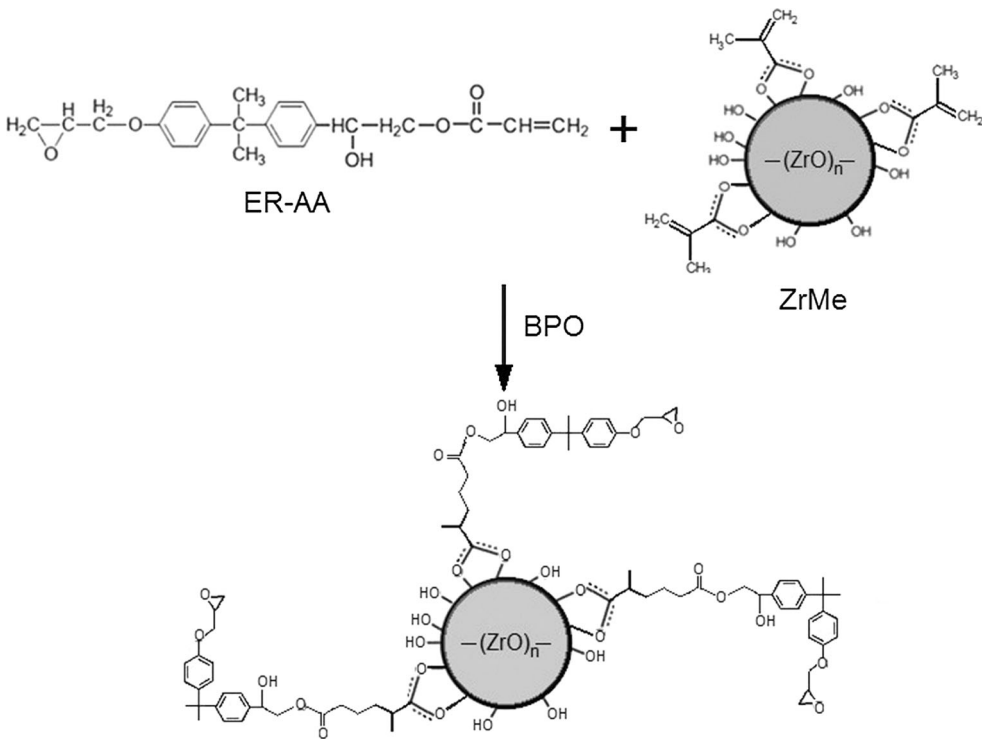

Fig. 8 Scheme for the free radical reaction between ER-AA and ZrMe oxocluster

networks prepared by method *IV* and cured with the anhydride/BPO system display the highest transparency (97 % with 5 phr of ZrMe oxocluster). This result is in agreement with the TEM observation and confirms the great dispersion of ZrMe when they were previously dispersed in anhydride.

The refractive index is also an important property for LED encapsulation applications. Therefore, this technique was also employed for characterizing the epoxy networks containing 5 phr of ZrMe oxocluster and prepared by different procedures, whose results are summarized in Table 3. All systems present a slight increase of the refractive index by the addition of the ZrMe oxocluster. The difference is not so significant because of the low amount of the zirconium oxide present in the systems. In fact, the amount of ZrO_2 in the ZrMe oxocluster is around 34 wt%, as presented by TGA, and the amount of ZrMe used in the composites corresponds to 5 part related to 100 part of epoxy resin. Considering that the overall composite is formed by 100 phr of epoxy resin, 100 phr of the curing agent (anhydride), and 5 phr of ZrMe, the actual amount of zirconium dioxide in the composites is around 0.90 wt%. This low amount of ZrO_2 explains the low increase of the refractive index in the epoxy-ZrMe hybrid materials. However, the best results have been achieved by method *IV* (where ZrMe was previously dispersed in the anhydride) due to the better dispersion of the ZrMe by this method, as confirmed by TEM and UV–Vis spectroscopy.

Viscoelasticity of the ER-AA/ZrMe nanocomposites The study related to the effect of the ZrMe content on the main dynamic mechanical properties of the ER-AA/ZrMe nanocomposites was performed with systems whose ZrMe was previously dispersed in the ER-AA (method *III*) or in the anhydride (method *IV*). The effect of the curing process, promoted by anhydride or by a combination of anhydride and BPO, was also investigated. Table 4 presents the main dynamic mechanical parameters of the ER-AA/ZrMe nanocomposites. The storage modulus generally increases as the amount of ZrMe increases, confirming the reinforcing effect of the ZrMe oxocluster. In fact, the use of only 1 wt% of ZrMe leads to an increase of around 20 % of the storage modulus and + 50 % for 5 wt% of ZrMe, regardless the dispersion method and the curing system used. The dispersion medium (ER-AA or anhydride) and the presence of BPO as the second curing agent do not significantly affect the modulus of the nanocomposites, except for the system containing 3 phr of ZrMe and cured with anhydride/BPO, whose oxoclusters were previously dispersed in anhydride. In this case, the modulus value reached value as high as 2600 MPa.

Contrarily to the modulus behavior, the medium where the oxoclusters have been previously dispersed exerts great influence on the glass transition temperature. Indeed, concerning the system prepared by method *III* and cured with anhydride, the T_g decreases as the amount of ZrMe increases. This phenomenon may be explained by the

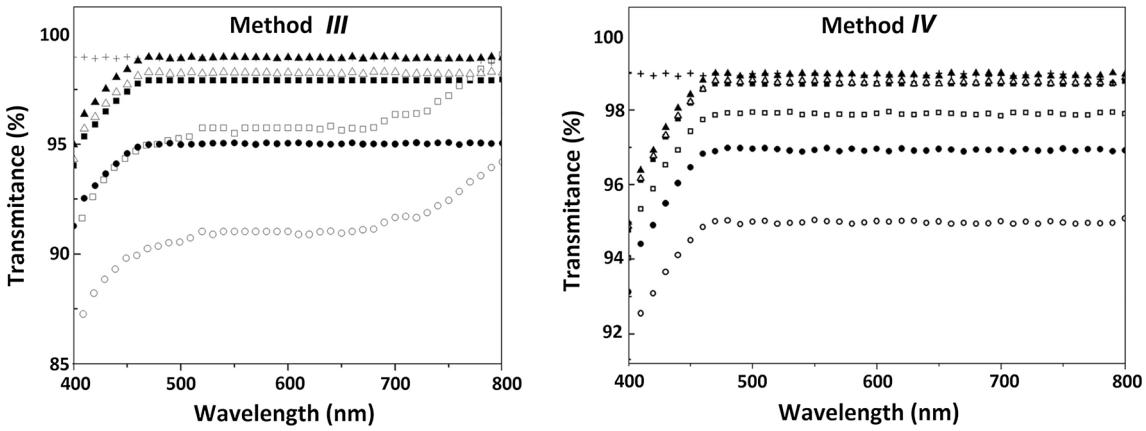

Fig. 9 UV–Vis spectra of ER-AA/ZrMe hybrid materials. *Plus sign* 0; *open triangle* 1; *open square* 3; and *open circle* 5 phr of ZrMe cured with anhydride and *filled triangle* 1; *filled square* 3; and *filled circle* 5 phr of ZrMe cured with anhydride/BPO

Table 3 Refractive index of ER-AA/ZrMe hybrid materials containing 5 phr of ZrMe, as a function of the preparative methodology

System	Curing system	Dispersion method	Refractive index
ER-AA	Anhydride	–	1.5519
ER-AA/ZrMe	Anhydride	Method *III*	1.5555
	Anhydride/BPO	Method *III*	1.5520
	Anhydride	Method *IV*	1.5629
	Anhydride/BPO	Method *IV*	1.5580

Table 4 Storage modulus and T_g of ER-AA/ZrMe nanocomposites as a function of the ZrMe content, dispersion method, and curing system

ZrMe content	Storage modulus (MPa)		T_g (°C)	
0	1600		124	
ZrMe content	Method *III*	Method *IV*	Method *III*	Method *IV*
Samples cured with anhydride				
1	1900	2100	125	122
3	2200	2200	118	121
5	2400	2300	114	129
Samples cured with anhydride/BPO				
1	1900	2000	135	139
3	2000	2600	138	141
5	2300	2400	138	135

mobility of the methacrylate groups at the surface of the ZrMe oxocluster. Additionally, the presence of free volume at the filler–matrix interface also contributes for the decrease of T_g. Systems whose ZrMe particles have been previously dispersed in the anhydride (method *IV*) generally display higher T_g, whose values increase with the ZrMe content. This behavior may be attributed to stronger interfacial adhesion probably through the formation of chelate complex between the carboxyl groups of the hydrolyzed anhydride and the remaining hydroxyl groups of the zirconium oxocluster, similarly to the mechanism proposed in the literature [16]. This phenomenon should decrease the free volume at the interface and also the chain mobility, which contribute for the increase in T_g. Systems cured with anhydride and BPO present a significant increase in T_g and those prepared by method *IV* display the highest values for systems containing 1 and 3 phr of ZrMe. These results are explained by the strong filler–matrix interaction through free radical reaction of the vinyl groups located in the epoxy matrix and at the ZrMe oxocluster surface, decreasing the mobility of these methacrylate groups.

Thermal conductivity Thermal conductivity in transparent polymer nanocomposites is also a very important property for LED applications and other electronic devices, since the overheating can decrease their shelf life. The through-plane thermal conductivity of the ER-AA/ZrMe hybrid materials, measured at different temperatures, was compared with that of epoxy network in Fig. 10. The presence of ZrMe resulted in a significant increase on the thermal conductivity related to the epoxy network. Systems prepared by method *III* display a slight decrease of the thermal conductivity with the increasing in temperature, whereas the thermal conductivity of systems prepared by method *IV* (ZrMe previously dispersed in anhydride) is independent on temperature for systems containing 3 and 5

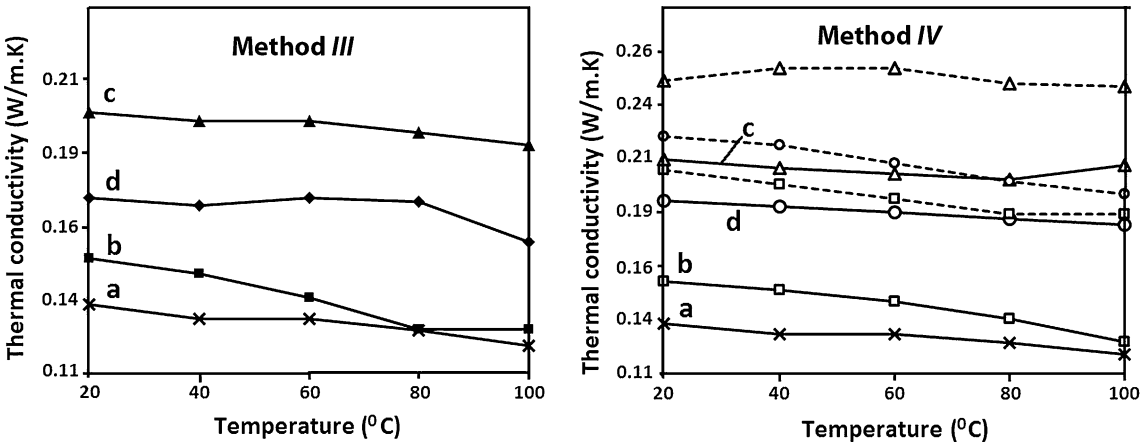

Fig. 10 Thermal conductivity of ER-AA/ZrMe hybrid materials. (*a*) 0; (*b*) 1; (*c*) 3; and (*d*) 5 phr of ZrMe cured with anhydride. The *dot lines* correspond to the samples cured with anhydride/BPO

phr of ZrMe. Additionally, these systems presented higher thermal conductivity, whose values increase considerably for systems cured with a combination of anhydride/BPO. At this condition, an increase of around 78 % (0.14–0.25 W/m K) was observed for the system containing 3 phr of ZrMe (which corresponds to 0.75 wt% of ZrO_2 as previously discussed). Similar behavior has been reported by Poostforush and Azizi [27] for crystallized anodic aluminum oxide impregnated with epoxy resin in a proportion of 33 vol% of filler. The excellent results achieved with ER-AA/ZrMe network cured with anhydride/BPO may be attributed to the better dispersion of the oxocluster inside the epoxy matrix, achieved by this procedure, as also observed by TEM. In this sense, the amount of 3 phr of ZrMe should provide a better dispersion. It is important to point out that this sample presented a transparency level close to the pure epoxy. This result is important because it is possible to increase significantly the thermal conductivity of the epoxy without losing the transparency, which is a very important characteristic for the development of several opto-electronic devices.

Conclusion

In this work, a new route to design inorganic–organic hybrids constituted by epoxy resin and methacrylate-zirconium oxoclusters (ZrMe) was described. Moreover, the optical and physical properties of the materials were investigated as a function of the ZrMe content, the medium where the ZrMe particles were previously dispersed and the curing system. For systems where the ZrMe particles were dispersed in the epoxy pre-polymer, the dispersion procedure based on a combination of high shear mechanical mixing and sonication resulted in better dispersion as indicated by the highest viscosity value and the highest storage modulus of the corresponding networked material obtained through dynamic mechanical analysis. Also the medium where the ZrMe particles were dispersed exerted strong influence on the morphology and main properties of corresponding nanocomposites. The ZrMe particles were dispersed as elongated flakes in systems prepared by method *III*. For systems prepared by method *IV*, a homogeneous distribution of the ZrMe nanoparticles was observed. For this dispersion procedure, samples cured with anhydride and BPO presented a very homogeneous morphology, and no discernible particle or aggregate could be observed even at higher magnification. This characteristic may be explained by the formation of chelates between the anhydride and the zirconium oxoclusters, which minimize the chance of particle aggregation and also to the action of peroxide, promoting covalent bonds between the epoxy matrix and the ZrMe oxoclusters through free radical addition involving the vinyl groups in both components. In conclusion, the combination of method *IV* for the previous dispersion of ZrMe and the use of anhydride together with BPO are the key parameters to obtain epoxy-zirconium nanocomposites with high glass transition temperature, high storage modulus, high optical transparency, and excellent thermal conductivity. Thus, these results open new possibilities of these hybrid materials as LED encapsulating materials and in other opto-electronic devices.

Acknowledgements This work was sponsored by the following Agencies in Brazil: Conselho Nacional de Desenvolvimento Científico e Tecnológico—CNPq, Financiadora de Estudos e Projetos—FINEP, and Fundação de Amparo à Pesquisa do Estado do Rio de Janeiro—FAPERJ. The authors acknowledge Dr. Annie Rivoire and Dr. Christelle Boule from Claude Bernard University for their help in microscopy.

References

1. Pascault JP, Williams RJJ (2010) Epoxy polymers: new materials and innovations. Wiley, Weinheim
2. Bourgeat-Lami E (2002) Organic-inorganic nanostructured colloids. J Nanosci Nanotechnol 2:1–24. doi:10.1166/jnn.2002.075
3. Sanchez C, Rozes L, Ribot F, Laberty-Robert C, Grosso D, Sassoye C, Boissiere C, Nicole L (2010) "Chimie douce": a land of opportunities for the designed construction of functional inorganic and hybrid organic-inorganic nanomaterials. CR Chim 13:3–39. doi:10.1016/qj.crci.2009.06.001
4. Tanaka K, Chujo Y (2012) Advanced functional materials based on polyhedral oligomeric silsesquioxane (POSS). J Mater Chem 22:1733–1746. doi:10.1039/c1jm14231c
5. Kango S, Kalia S, Celli A, Njuguna J, Habibi Y, Kumar R (2013) Surface modification of inorganic nanoparticles for development of organic-inorganic nanocomposites—a review. Prog Polym Sci 38:1232–1261. doi:10.1016/j.progpolymsci.2013.02.003
6. Schmidt H (2006) Considerations about the sol-gel process: from the classical sol-gel route to advanced chemical technologies. J Sol Gel Sci Technol 40:115–130. doi:10.1007/s10971-006-9322-6
7. Kumani L, Du GH, Li WZ, Vennila RS, Saxena SK, Wang DZ (2009) Synthesis, microstructure and optical characterization of zirconium oxide nanostructures. Ceram Int 35:2401–2408. doi:10.1016/j.ceramint.2009.02.007
8. Yang S, Kwak SY, Jin J, Kim JS, Choi Y, Paik KW, Bae BS (2012) Thermally resistant UV-curable epoxy-siloxane hybrid materials for light emitting diode (LED) encapsulation. J Mater Chem 22:8874–8880. doi:10.1039/C2JM16355A
9. Tao P, Li Y, Siegel RW, Schadler LS (2013) Transparent dispensible high-refractive index ZrO_2/epoxy nanocomposites for LED encapsulation. J Appl Polym Sci 130:3785–3793. doi:10.1002/app.39652
10. Medina R, Haupert F, Schlarb AK (2008) Improvement of tensile properties and toughness of an epoxy resin by nanozirconium-dioxide reinforcement. J Mater Sci 43:3245–3252. doi:10.1007/s10853-008-2547-8
11. Sajjad M, Feichtenschlager B, Pabisch S, Svehla J, Koch T, Seidler S, Peterlik H, Kickelbick G (2012) Study of the effect of the concentration, size and surface chemistry of zirconia and silica nanoparticle fillers within an epoxy resin on the bulk properties of the resulting nanocomposites. Polym Int 61:274–285. doi:10.1002/pi.3183
12. Bondioli F, Cannillo V, Fabbri E, Messori M (2006) Preparation and characterization of epoxy resins filled with submicron spherical zirconia particles. Polimery 51:794–798
13. Dorigato A, Pegoretti A, Bondioli F, Messori M (2010) Improving epoxy adhesives with zirconia nanoparticles. Compos Interfaces 17:873–881. doi:10.1163/092764410X539253
14. Ochi M, Nii D, Suzuki Y, Harada M (2010) Thermal and optical properties of epoxy/zircônia hybrid materials synthesized via in situ polymerization. J Mater Sci 45:2655–2661. doi:10.1007/s10853-010-4244-7
15. Ochi M, Nii D, Harada M (2010) Effect of acetic acid content on in situ preparation of epoxy/zirconia hybrid materials. J Mater Sci 45:6159–6165. doi:10.1007/s10853-010-4702-2
16. Ochi M, Nii D, Harada M (2011) Preparation of epoxy/zirconia hybrid materials via in situ polymerization using zirconium alkoxide coordinated with acid anhydride. Mater Chem Phys 125:424–432. doi:10.1016/j.matchemphys.2011.04.034
17. Bondioli F, Darecchio ME, Luyt AS, Messori M (2011) Epoxy resin modified with in situ generated metal oxides by means of sol-gel process. J Appl Polym Sci 122:1792–1799. doi:10.1002/app.34264
18. Chung PT, Yang CT, Wang SH, Chen CW, Chiang AST, Liu CY (2012) ZrO_2/epoxy nanocomposite for LED encapsulation. Mater Chem Phys 136:868–876. doi:10.1016/j.matchemphys.2012.08.013
19. Schubert U (2004) Organofunctional metal oxide clusters as building blocks for inorganic-organic hybrid materials. J Sol Gel Sci Technol 31:19–24
20. Moraru B, Kickelbick G, Schubert U (2001) Methacrylate-substituted mixed-metal clusters derived from zigzag chains of $[ZrO_8]/[ZrO_7]$ and $[TiO_6]$ polyhedra. Eur J Inorg Chem 2001:1295–1301
21. Trimmel G, Gross S, Kickelbick G, Schubert U (2001) Swelling behavior and thermal stability of poly(methylmethacrylate) crosslinked by the oxozirconium cluster $Zr_4O_2(methacrylate)_{12}$. Appl Organomet Chem 15:401–406. doi:10.1002/aoc.161
22. Kickelbick G, Wiede P, Schubert U (1999) Variations in capping the $Zr_6O_4(OH)_4$ cluster core: X-ray structure analyses of $[Zr_6(OH)_4O_4(OOC\text{-}CH{=}CH_2)_{10}]_2(\mu\text{-}OOC\text{-}CH{=}CH_2)_4$ and $Zr_6(OH)_4O_4(OOCR)_{12}(PrOH)$ (R=Ph, $CMe{=}CH_2$). Inorg Chim Acta 284:1–7
23. Asiltürk M, Burunkaya E, Sayilkan F, Kiraz N, Arpaç E (2011) J. Non Cryst Solids 357:206–210. doi:10.1016/j.jnoncrysol.2010.09.034
24. Kotsilkova R (2005) Processing-structure-properties relationships of mechanically and thermally enhanced smectite/epoxy nanocomposites. J Appl Polym Sci 97:2499–2510. doi:10.1002/app.21989
25. Sternstein SS, Ramorino G, Jiang B, Zhu A (2005) Reinforcement and nonlinear viscoelasticity of polymer melts containing mixtures of nanofillers. Rubber Chem Technol 78:258–270. doi:10.5254/1.3547882
26. Galgali G, Ramesh C, Lele A (2001) A rheological study on the kinetics of hybrid formation of polypropylene nanocomposites. Macromolecules 34:852–858. doi:10.1021/ma000565f
27. Pootforush M, Azizi H (2014) Superior thermal conductivity of transparent polymer nanocomposites with a crystallized alumina membrane. Express Polym Lett 8:293–299. doi:10.3144/expresspolymlett.2014.32